Cellular and Molecular Life Sciences (2023) 80:200
https://doi.org/10.1007/s00018-023-04847-z

ORIGINAL ARTICLE

Artificial induction of circadian rhythm by combining exogenous BMAL1 expression and polycomb repressive complex 2 inhibition in human induced pluripotent stem cells

Hitomi Kaneko[1] · Taku Kaitsuka[2] · Kazuhito Tomizawa[1]

Received: 15 March 2023 / Revised: 22 June 2023 / Accepted: 26 June 2023 / Published online: 8 July 2023

Abstract

Understanding the physiology of human-induced pluripotent stem cells (iPSCs) is necessary for directed differentiation, mimicking embryonic development, and regenerative medicine applications. Pluripotent stem cells (PSCs) exhibit unique abilities such as self-renewal and pluripotency, but they lack some functions that are associated with normal somatic cells. One such function is the circadian oscillation of clock genes; however, whether or not PSCs demonstrate this capability remains unclear. In this study, the reason why circadian rhythm does not oscillate in human iPSCs was examined. This phenomenon may be due to the transcriptional repression of clock genes resulting from the hypermethylation of histone H3 at lysine 27 (H3K27), or it may be due to the low levels of brain and muscle ARNT-like 1 (BMAL1) protein. Therefore, BMAL1-overexpressing cells were generated and pre-treated with GSK126, an inhibitor of enhancer of zest homologue 2 (EZH2), which is a methyltransferase of H3K27 and a component of polycomb repressive complex 2. Consequently, a significant circadian rhythm following endogenous *BMAL1*, *period 2* (*PER2*), and other clock gene expression was induced by these two factors, suggesting a candidate mechanism for the lack of rhythmicity of clock gene expression in iPSCs.

Keywords iPSCs · Circadian rhythm · BMAL1 · GSK126 · PRC2 · H3K27 me3

Introduction

Pluripotent stem cells (PSCs) as embryonic stem cells (ESCs) and induced pluripotent stem cells (iPSCs) are characteristic cells that can indefinitely proliferate and differentiate into a variety of cells in the body. Thus, the expression of pluripotency and differentiation genes is strictly controlled in PSCs through epigenetic mechanisms, such as DNA methylation and histone modifications. Conversely, PSCs lack several functions, including circadian rhythm [1, 2], resistance to proteotoxicity [3], and replicative senescence [4, 5], which are normally exhibited by somatic cells.

Circadian rhythm is necessary for cellular homeostasis and the health of an organism [6]. Molecular clocks, which induce circadian rhythmicity, exist in most cells of the body, and they are regulated by clock genes and transcription/translation feedback loops [7]. In mammals, peripheral organs express molecular clocks that are synchronized by fasting–feeding cycles and inputs from the central clock, which is controlled by light–dark cycles through the suprachiasmatic nucleus in the hypothalamus [8]. Fluctuation of mammalian body temperature from 2 to 3 °C during the day also synchronizes clock gene expression [9].

In PSCs, researchers showed that circadian rhythm associated with clock gene expression is not induced in mouse and human ESCs or iPSCs [1, 2, 10, 11]. Why PSCs do not express this rhythm machinery is gradually elucidated but not fully cleared. In mouse ESCs, Umemura et al. demonstrated that the development of a differentiation-coupled circadian clock is disrupted by the misregulation of Importin-α2, which regulates the subcellular localization of period 1 (PER1) and PER2 proteins [12]. Furthermore, the

✉ Taku Kaitsuka
kaitsuka@iuhw.ac.jp

✉ Kazuhito Tomizawa
tomikt@kumamoto-u.ac.jp

[1] Department of Molecular Physiology, Faculty of Life Sciences, Kumamoto University, 1-1-1 Honjo, Chuo-Ku, Kumamoto 860-8556, Japan

[2] School of Pharmacy at Fukuoka, International University of Health and Welfare, Enokizu 137-1, Okawa, Fukuoka 831-8501, Japan

CLOCK protein is not found despite the expression of its mRNA in mouse ESCs and human iPSCs, and the posttranscriptional regulation of CLOCK is required for the emergence of circadian clock oscillation during development [1, 13]. Although such studies have shown the mechanism of differentiation-coupled circadian clock development, the circadian clock in PSCs has not been induced by keeping an undifferentiated state. The clock genes, namely, *PERs*, *cryptochromes* (*CRYs*), *circadian locomoter output cycles protein kaput* (*CLCOK*), and *brain and muscle ARNT-like 1* (*BMAL1*), are expressed in PSCs; however, their circadian oscillation could be repressed by unknown mechanisms. In general, the steady-state and stimulus-responsive expression of developmental genes are epigenetically repressed in PSCs. The methylation of lys27 on histone H3 (H3K27) is a major repressive modification and a hallmark of facultative heterochromatin [14]. H3K27 methylation is catalyzed by an enhancer of zest homologue 2 (EZH2) of polycomb repressive complex 2 (PRC2). In PSCs, H3K27 me3 is located at the promoters of many important developmental regulators [15]; however, the regulation of clock genes by PRC2 has not been examined. The induction of circadian rhythm may not occur because of such epigenetic repressive effects, and the mRNA and protein levels of BMAL1 are lower in human iPSCs compared with U2OS cells, which normally have a circadian clock [16]. BMAL1 is a transcription factor that binds to the E-boxes of *PER1*, *PER2*, *CRY1*, and *CRY2*, and it activates their transcription with the CLOCK protein. Therefore, BMAL1 is essential for rhythm generation, which is supported by evidence that *Bmal1*-deficient mice become immediately arrhythmic under constant darkness [17, 18].

In this study, the mechanism of the repression of molecular clock oscillation in human iPSCs was determined, and the circadian rhythm of clock genes was induced by artificially expressing BMAL1 and treating with a PRC2 inhibitor, GSK126.

Results

Hypermethylation of H3K27 in the *PER1* promoter in human iPSCs

In our previous study, the early induction of *PER1* by dexamethasone (Dex) and forskolin (Frk) treatments did not occur in human iPSCs, and the circadian rhythm of the clock gene expression was not evident. Initially, we focused on the methylation of H3K27 in the *PER1* promoter, which is a major repressive histone modification in PSCs. Based on the GSE107176 dataset in the NCBI database submitted by Chan et al., iPSCs exhibit higher H3K27 me3 levels around the transcription start site (TSS) of *PER1*, *PER2*, *PER3*, and *BMAL1* than MCF10A cells, a human breast epithelial cell line, indicating that the transcription of these genes is epigenetically repressed (Suppl. Fig. S1) [19]. The active mark of H3K4 me3, which is regulated by the Trithorax group (TrxG), is also distributed in *PER1*, *PER2*, *PER3*, and *BMAL1* TSS of iPSCs. These data indicate that the epigenetic status of these genes is bivalent, which is a unique characteristic of genes involved in the differentiation and development of PSCs [20]. H3K27ac is distributed in the TSS, and the enhancer region of transcriptionally active genes [21] and the expression level of *PER1*, *PER2*, and *BMAL1* in iPSCs were lower than those in MCF10A cells (Suppl. Fig. S1). The epigenetic status of these genes is similar to the *HOXA* cluster, a target of PRC2 (Suppl. Fig. S1). Conversely, a pluripotency gene, *NANOG*, exhibited higher H3K27ac levels in iPSCs (Suppl. Fig. S1). Other clock genes, such as *CLOCK*, *CRY1*, and *CRY2*, did not show any peaks of H3K27 me3 in their TSS (Suppl. Fig. S1). Next, the H3K27 me3 status in clock genes on multiple lines of iPSCs was analyzed using the GSE165869 dataset submitted by Yokobayashi et al. [22]. This modification was enriched in the upstream of *PER1* TSS in almost all iPSC lines induced from male or female somatic cells (Suppl. Fig. S2). However, no evident peaks were observed in the TSS of other clock genes, including *PER2* and *BMAL1*, whereas apparent peaks of H3K27 me3 were observed in the *HOXA* cluster (Suppl. Fig. S2). In human ESCs, a gold standard of human PSC, higher H3K27 levels were observed in the TSS of *PER1* and *BMAL1* genes when analyzed by using the GSE145964 dataset [23] compared with *PER2* and other genes (Suppl. Fig. S3). Furthermore, in this dataset, researchers compared iPSCs with its differentiated cells, including neural stem cell (NSC), vascular endothelial cell, vascular smooth muscle cell, and mesenchymal stem cell. In addition, low levels of H3K27ac in the TSS of *PER1*, *PER2*, and *BMAL1* were found in ESCs and iPSCs, whereas these levels remarkably increased in differentiated cells, showing that the epigenetic state of some clock genes activates during differentiation (Suppl. Fig. S3).

Based on these findings, the methylation status of H3K27 around the TSS of *PER1* in iPSC line 201B7 and U2OS cells was examined using a chromatin immunoprecipitation (ChIP) assay followed by quantitative PCR analysis with primers specific for the upstream and downstream regions of the TSS. The human osteosarcoma cell line U2OS is appropriately controlled to study the human clock, which expresses circadian clock components that drive the oscillation of core clock genes [24]. The results indicated that 201B7 iPSCs exhibited higher H3K27 me3 and lower H3K27ac levels around the TSS of *PER1* than U2OS cells (Fig. 1A).

In determining whether the methylation of H3K27 in *PER1* results from PRC2, 201B7 iPSCs were treated with GSK126, an inhibitor of the histone methyltransferase

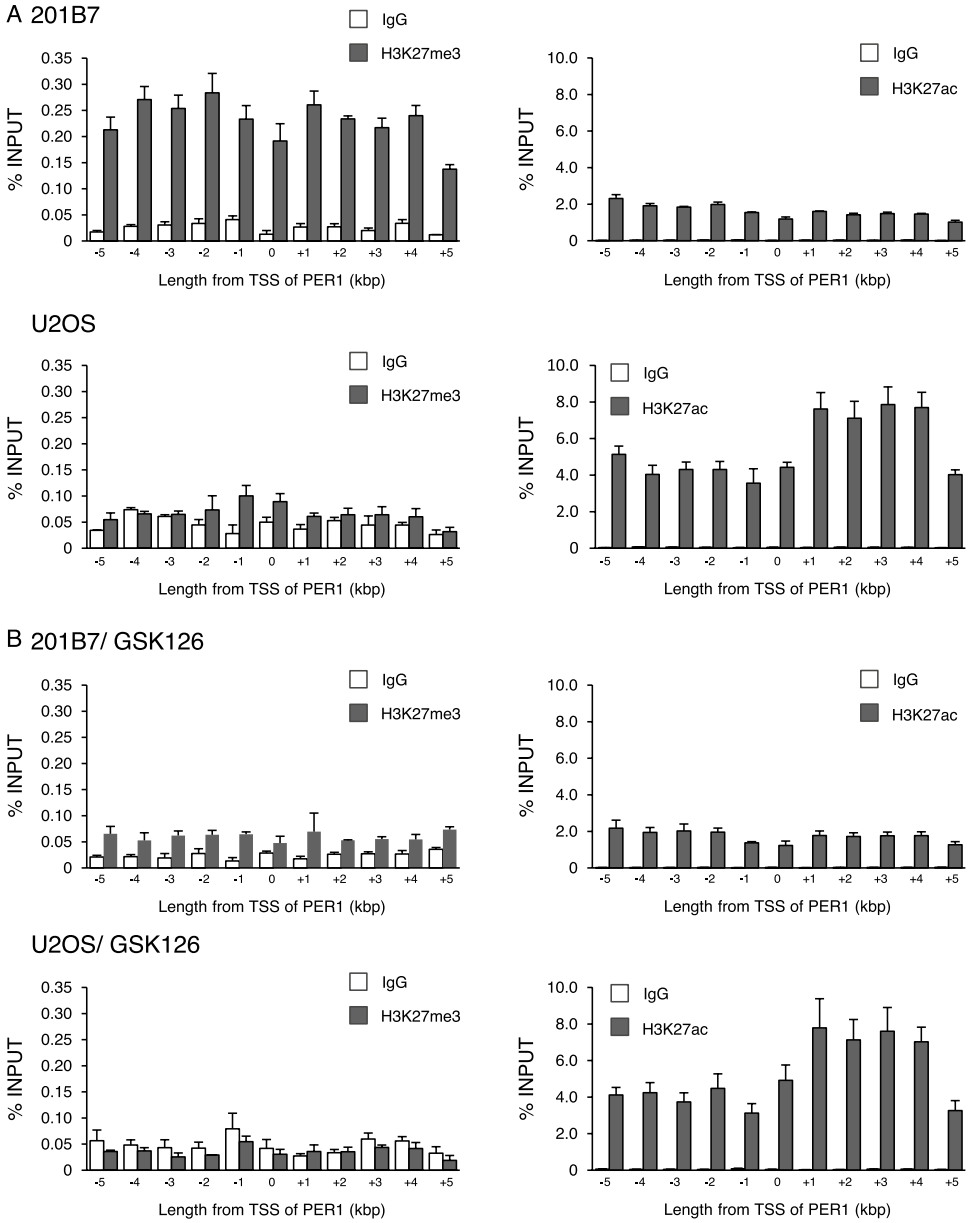

Fig. 1 H3K27 modification around the transcription start site (TSS) of *PER1* in iPSCs and U2OS cells. **A, B** ChIP-qPCR analysis of H3K27 me3 and H3K27ac. The percentage of each precipitated DNA fragment around the TSS of *PER1* by anti-H3K27 me3 and H3K27ac antibodies to INPUT was analyzed in 201B7 iPSCs and U2OS cells in a steady-state (**A**) or after treatment with 5 μM GSK126 for 48 h (**B**). The 0 on the *x*-axis indicates the 200-bp region around the TSS. + 1 to + 5 and − 1 to − 5 on the *x*-axis indicate the 200-bp region around 1–5 kbp upstream or downstream of the TSS, respectively. Data are presented as means ± SEM; $n = 3$ from independent experiments for each comparison

EZH2, which inhibits the methylation of H3K27 [25]. H3K27 me3 levels in iPSCs were markedly higher than those in U2OS cells, and GSK126 treatment significantly reduced methylation levels at a concentration of 5 and 10 μM (Suppl. Figs. S4A and B). The time course of the inhibition of H3K27 methylation by GSK126 was assessed, and the result showed that treatment for more than 2 days markedly repressed total H3K27 me3 levels (Suppl. Fig. S4C). Of the H3K27 me3 around the TSS of *PER1*, treatment with 5 μM GSK126 for 48 h reduced the levels in 201B7 iPSCs but not in U2OS cells (Fig. 1B). Next, similar results were obtained following treatment with GSK126, which also reduced H3K27 me3 levels around the TSS of *BMAL1* and *PER2* (Suppl. Figs. S5 and 6). 201B7 originated from female dermal fibroblast [26]. Therefore, the status of histone marks in the 1383D6 line was tested using its origin of male human dermal fibroblast (HDF) as somatic control to analyze another iPSC line of male origin [27]. H3K27 me3 modification levels were enriched around the TSS of *PER1*, *PER2*, and *BMAL1*, and then they were repressed by GSK126 treatment (Suppl. Figs. S7–9). Although HDF also had high levels of H3K27 me3 in those genes, their levels were not remarkably affected by GSK126 treatment (Suppl. Figs. S7–9). Furthermore, acetylated levels of H3K27 were higher in HDF than 1383D6, which is similar to the comparison results between 201B7 and U2OS cells (Suppl. Figs. S7–9). These data indicate that the expression level of *PER1*, *PER2*, and *BMAL1* is epigenetically repressed by PRC2

in iPSCs. However, the levels of H3K27ac in these genes remained unchanged by EZH2 inhibition (Fig. 1B, Suppl. Figs. S5 and 6).

Clock gene expression in iPSCs with or without GSK126 treatment

EZH2 inhibition could circumvent the repression of gene transcription by inhibiting H3K27 methylation. Therefore, changes in the expression of clock genes in iPSCs were examined following GSK126 treatment. However, no significant differences were found in *D-box-binding protein* (*DBP*), *BMAL1*, *CLOCK*, *PER1*, *PER2*, *PER3*, *CRY1*, *CRY2*, *nuclear receptor subfamily 1 group D member 1* (*NR1D1*), *NR1D2*, *retinoic acid receptor related orphan receptor A* (*RORA*), or *RORB* between vehicle (dimethyl sulfoxide, DMSO) and GSK126-treated 201B7 iPSCs (Fig. 2A). This discrepancy might be due to low levels of H3K27ac even after GSK126 treatment. Thus, the histone deacetylase inhibitor trichostatin A (TSA) was added to cells after GSK126 treatment, and *PER1*, *PER2*, and *BMAL1* expression levels were measured. Consequently, their levels significantly increased by GSK126 in the presence of TSA (Suppl. Fig. S10). Next, the induction of *PER1* expression in response to synchronizing agents during GSK126 treatment was assessed. The results indicated that *PER1* expression was not induced by Dex or Frk stimulation even with concurrent GSK126 treatment (Fig. 2B).

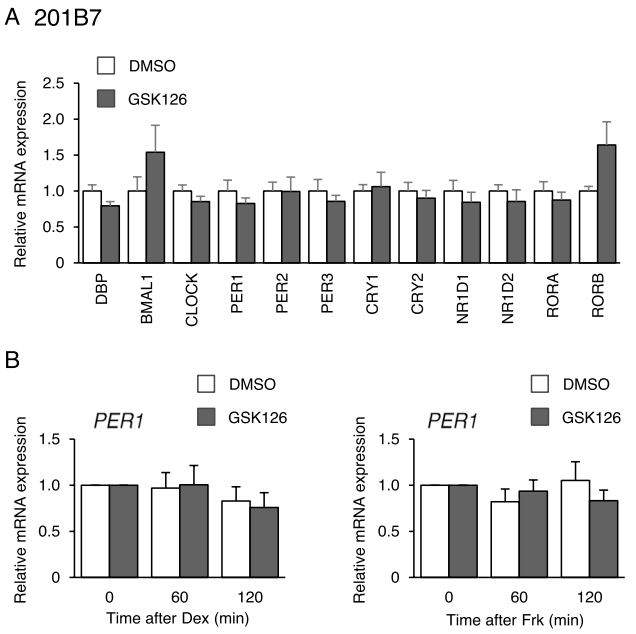

Fig. 2 Effect of GSK126 treatment on clock gene expression in iPSCs. **A** Expression level of clock genes was measured in 201B7 iPSCs treated with DMSO or 5 μM GSK126 for 48 h. Data are presented as means ± SEM relative to DMSO-treated cells; $n = 6$ for independent experiments for each comparison. **B** The expression level of *PER1* was measured after the stimulation of Dex and Frk in 201B7 iPSCs pre-treated with DMSO or 5 μM GSK126 for 48 h. Data are presented as means ± SEM relative to each 0 min; $n = 6$ for independent experiments for each comparison

Increased clock gene expression by the overexpression of BMAL1 in iPSCs

As previously reported, the level of *BMAL1* gene expression and its protein in 201B7 iPSCs was significantly lower than that in U2OS cells [16]. Similar results were obtained in the expression level of *BMAL1* and *CLOCK* mRNA among various iPSC lines with somatic fibroblasts as control (Suppl. Fig. S11A). At the protein level, although CLOCK levels were relatively lower in iPSC lines than each fibroblast, BMAL1 levels were not remarkably different from them (Suppl. Fig. S11B). Based on our present and previous results, fibroblasts have lower levels of BMAL1 protein than U2OS cells. From the GSE16654 dataset [28], the expression levels of *BMAL1* and *CLOCK* were similar between several iPSC lines and ESCs (Suppl. Fig. S11C). Based on the previous insight obtained from the comparison between iPSCs and U2OS cells, a stable cell line expressing exogenous BMAL1 was established to enhance the response to synchronizing agents in iPSCs. The resulting cell line (201B7-BMAL1) exhibited high levels of BMAL1 protein, which was similar to U2OS cells (Fig. 3A). The expression levels of the *CLOCK*, *PER1-3*, *CRY1,2*, *DBP*, and *NR1D* genes were significantly higher in 201B7-BMAL1 cells than in control 201B7 iPSCs (Fig. 3B). Next, the early induction of *PER1* by Dex and Frk stimulation in this cell line was examined; however, no significant response was observed in 201B7-BMAL1 cells (Fig. 3C).

Induction of the circadian oscillation of *PER2* and *BMAL1* expression in 201B7-BMAL1 treated with GSK126

The early induction of *PER1* by Dex and Frk did not occur in iPSCs with neither GSK126 treatment nor BMAL1 overexpression. Therefore, 201B7-BMAL1 cells were treated with GSK126, and the early induction of *PER1* was examined, as both factors were exposed simultaneously. Consequently, a significant increase of *PER1* was observed 60 min after Dex stimulation and 120 min after Frk exposure (Fig. 4A). However, no significant changes were found in the expression of clock genes between DMSO and GSK126 treatment in 201B7-BMAL1 (Fig. 4B).

Next, whether GSK126-treated 201B7-BMAL1 cells showed a circadian rhythm of clock gene expression was verified. 201B7-BMAL1 without GSK126 treatment did not show a significant rhythm in the expression of *PER2* and endogenous *BMAL1*, which was detected using primers

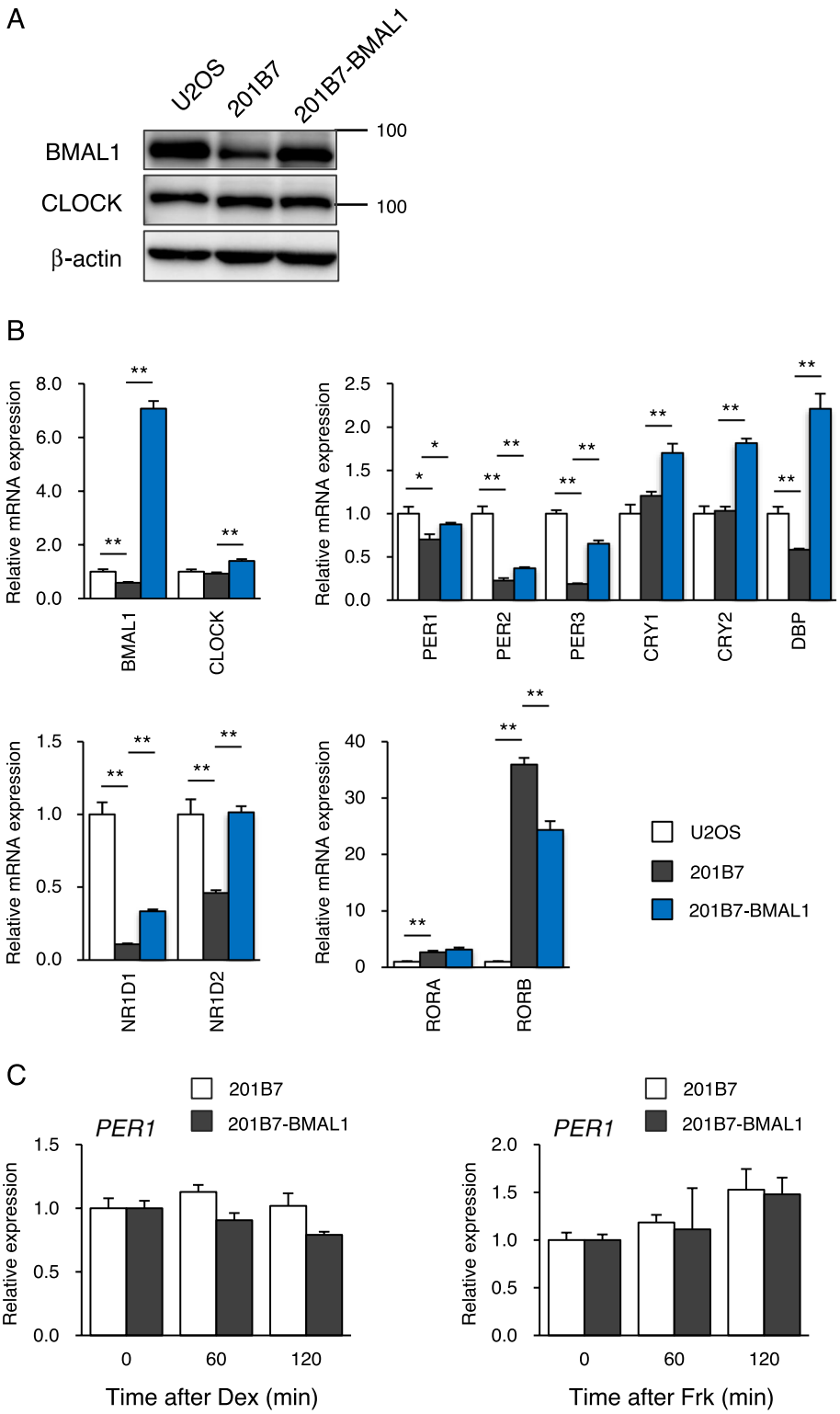

Fig. 3 Clock gene expression in BMAL1-overexpressing iPSCs. **A** BMAL1 and CLOCK protein levels were measured in U2OS cells, 201B7 iPSCs, and 201B7-BMAL1. β-actin levels were used as a loading control. **B** Expression levels of clock genes were measured in U2OS cells, 201B7 iPSCs, and 201B7-BMAL1. Next, data are presented as means ± SEM relative to U2OS cells; $n = 3$ for independent experiments for each comparison. $^{*}P < 0.05$, $^{**}P < 0.01$ versus each value of 201B7 iPSCs. **C** The expression level of *PER1* was measured after the stimulation of Dex and Frk in 201B7 iPSCs and 201B7-BMAL1. Data are presented as mean ± SEM relative to each 0 min; $n = 3$ for independent experiments for each comparison

designed within the 3′ untranslated region (UTR) after Dex and Frk stimulations (Fig. 5A, B). In GSK126-treated 201B7-BMAL1 cells, a statistically significant circadian rhythm of *PER2* and endogenous *BMAL1* expression was observed at 0–24 h following Dex stimulation (Fig. 5A). In addition, a significant circadian rhythm of *PER2* was observed at 0–24 h following Frk stimulation (Fig. 5B). The expression of exogenous *BMAL1* was not rhythmic under any treatment, which was detected using primers designed within the FLAG tag (Fig. 5A, B). At 0–48 h after synchronization,

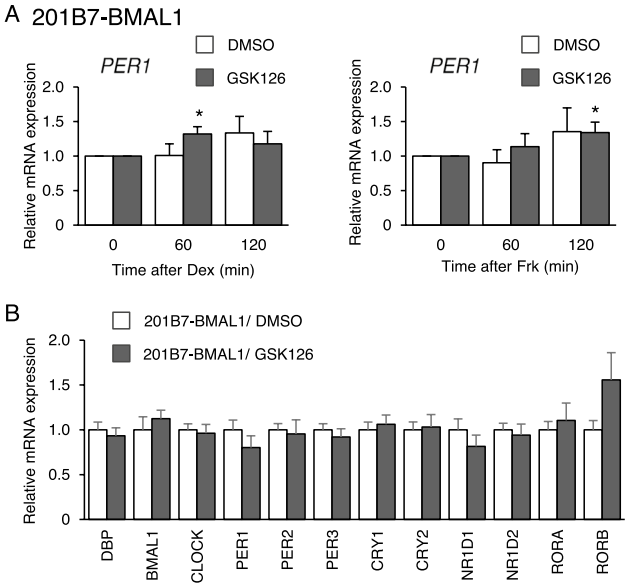

Fig. 4 Effect of GSK126 treatment on clock gene expression in BMAL1-overexpressing iPSCs. **A** The expression level of *PER1* was measured after the stimulation of Dex and Frk in 201B7-BMAL1 pretreated with DMSO or 5 μM GSK126 for 48 h. Next, data are presented as means ± SEM relative to each 0 min; $n=6$ for independent experiments for each comparison. $^*P<0.05$ versus the corresponding control at 0 min. **B** Expression levels of the clock genes were measured in 201B7-BMAL1 cells treated with DMSO or 5 μM GSK126 for 48 h. Next, data are presented as means ± SEM relative to DMSO-treated 201B7-BMAL1; $n=6$ for independent experiments for each comparison

statistically significant rhythms of *PER2*, *CRY1*, and *PER1* expression by Dex and *PER2* as well as *CRY1* expression by Frk were also observed in 201B7-BMAL1 with GSK126 treatment (Suppl. Fig. S12A). For another iPSC line of male origin, 1383D6-expressing exogenous BMAL1 (Suppl. Fig. S12C) was prepared, and the circadian expression of clock genes was tested. In the absence of GSK126 treatment, the circadian rhythm of *PER2* expression was detected after Dex stimulation (Suppl. Fig. S12B). With GSK126 treatment, the expression of *CLOCK* and *CRY1* showed a significant rhythm in addition to *PER2* (Suppl. Fig. S12B).

With regard to the modification of H3K27, GSK126 treatment decreased H3K27 me3 levels and increased acetylation around the TSS of *PER1* in 201B7-BMAL1 cells (Fig. 6A). Furthermore, GSK126 treatment decreased H3K27 me3 levels and increased H3K27ac levels around the TSS of *BMAL1* (Fig. 6B).

GSK126 treatment and BMAL1 overexpression affect the proliferation ability but not pluripotency of iPSCs

Finally, whether GSK126 treatment and BMAL1 overexpression maintained the pluripotency of iPSCs was determined. Consequently, the expression level of the naïve markers *KLF4* and *DNMT3L* as well as the primed marker *ZIC3* slightly increased with BMAL1 overexpression in DMSO and GSK126 treatment (Fig. 7A), whereas no remarkable changes (over 1.5-fold) in pluripotency markers were observed among all groups (Fig. 7A). In addition, immunofluorescence analysis showed that almost all cells express Oct4 protein in all groups (Suppl. Fig. S13A). By flow cytometry analysis, most 201B7-BMAL1 cells expressed SSEA-4, a pluripotency marker, and EZH2 inhibition by GSK126 did not change the percentage of SSEA-4-positive cells, indicating that pluripotency was maintained (Fig. 7B). However, when the proliferation capacity was examined, BMAL1 overexpression significantly repressed the proliferation rate of 201B7 iPSCs with and without GSK126 treatment (Fig. 7C). The reduced proliferation of 201B7-BMAL1 with and without GSK126 was not due to increased apoptosis when assessed by annexin V staining (Suppl. Fig. S13C). Then, the differentiation capacity of those cells was tested on the basis of the formation of embryoid bodies (EBs). After 18 days of EB formation, the pluripotency of marker genes OCT4 and NANOG remarkably decreased in 201B7 iPSCs and 201B7-BMAL1 with and without GSK126, respectively (Fig. 8). In 201B7 iPSCs, the number of EBs in endoderm markers SOX17 and GATA4, mesoderm markers T and MESP1, and ectoderm markers SOX1 and FGF5 significantly increased, showing that these cells were differentiated into three germ layers. 201B7-BMAL1 cells treated with GSK126 had increased levels of those markers, whereas they expressed lower levels of mesoderm marker genes than 201B7 iPSCs, indicating that the differentiation tendency to each germ layer was slightly affected by both treatments. After 15 passages, 201B7-BMAL1 with GSK126 treatment maintained similar expression levels of pluripotency markers to 201B7 iPSCs (Suppl. Fig. S13B).

Discussion

In general, the regulation of cell physiology by circadian rhythm occurs during development, and undifferentiated cells, such as ESCs and iPSCs, lack such machinery. These cells also do not need such a machinery for their physiological functions. In the present study, low levels of BMAL1 and epigenetic repression of clock genes by histone modification of H3K27 me3 suppress the emergence of circadian rhythms in PSCs. Furthermore, rhythms were artificially induced by overexpressing BMAL1 and inhibiting EZH2, a component of PRC2.

PRC2 represses developmental genes, such as *Hox* (which control the body plan), *Sox*, *Pax*, *Evx*, and *Otx*, through bivalent histone modification with active mark H3K4 me3 [29, 30]. In human PSCs, development commitment genes

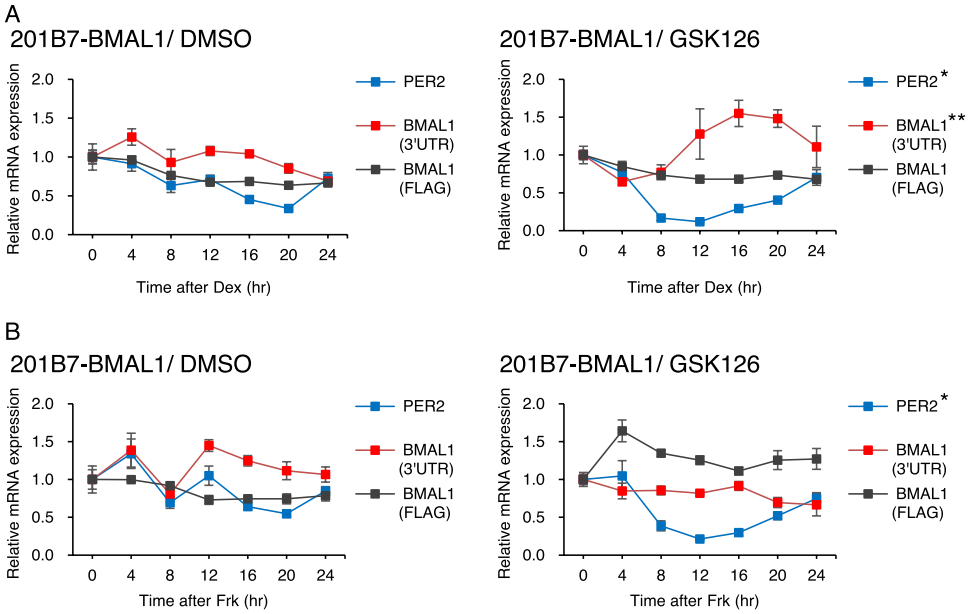

Fig. 5 Induction of the circadian oscillation of *PER2* and *BMAL1* expression in iPSC-BMAL1 cells treated with GSK126. **A** *PER2*, endogenous (3′UTR) and exogenous (FLAG) *BMAL1* expression was measured every 4 h after Dex stimulation in 201B7-BMAL1 cells treated with DMSO or 5 μM GSK126 for 48 h. Data are presented as means ± SEM relative to 0 h; $n=3$ for each comparison. *P* values for the rhythmicity of *PER2* and *BMAL1* were determined by cosinor analysis as $P=0.187$ (*PER2*), $P=0.589$ (*BMAL1* 3′UTR), and $P=0.271$ (*BMAL1* FLAG) in iPSC-BMAL1 with DMSO and $P=0.027$ (*PER2*), $P=0.00027$ (*BMAL1* 3′UTR), and $P=0.370$ (*BMAL1* FLAG) in 201B7-BMAL1 with GSK126, respectively. **B** *PER2*, endogenous (3′UTR) and exogenous (FLAG) *BMAL1* expression was measured every 4 h after Frk stimulation in 201B7-BMAL1 treated with DMSO or 5 μM GSK126 for 48 h. Data are presented as means ± SEM relative to 0 h; $n=3$ for each comparison. *P* values for the rhythmicity of *PER2* and *BMAL1* were determined by cosinor analysis as $P=0.349$ (*PER2*), $P=0.798$ (*BMAL1* 3′UTR), and $P=0.098$ (*BMAL1* FLAG) in 201B7-BMAL1 cells with DMSO and $P=0.018$ (*PER2*), $P=0.870$ (*BMAL1* 3′UTR), and $P=0.363$ in 201B7-BMAL1 cells with GSK126, respectively

(e.g., *GATA2*, *CDX2*, *PAX6*, and *GATA6*) were also in a bivalent state with H3K4 me3 and H3K27 me3 modifications, whereas the pluripotency genes *NANOG* and *POU5F1* showed an H3K4 me3 state without H3K27 me3 [31]. In somatic cells, these developmental genes are activated without H3K27 me3 modification [32]. In the present study, the expression level of the clock gene *PER1* was regulated by H3K27 me3 modification in human iPSCs because the EZH2 inhibitor, GSK126, significantly reduced the level of modification. This effect was confirmed by two iPSC lines, namely, 201B7 and 1383D6, originated from somatic female and male cells, respectively. Studies regarding the epigenetic state of the clock genes in PSCs are limited. Etchegaray et al. showed that EZH2 binds to the promoters *Per1* and *Per2* and methylates H3 at K27 in mouse liver [33]. In PSCs, no reports exist regarding clock gene regulation by PRC2; therefore, this study is the first to report that PRC2 might be involved in the epigenetic regulation of *PER1* in human iPSCs. On the contrary, the level of H3K27 me3 in *PER1*, *PER2*, and *BMAL1* of U2OS cells and HDFs is not remarkably reduced by GSK126 (Fig. 1 and Suppl. Figs. S5–9). In general, EZH2 is highly expressed in PSCs, and its expression level subsequently declines throughout differentiation, whereas the expression level of EZH1, another catalytic subunit of PRC2, gradually increases [34, 35]. Therefore, GSK126, a selective inhibitor of EZH2, may less affect H3K27 me3 modification in such somatic cells because of the shift of the PRC2 component from PRC2/EZH2 to PRC2/EZH1. However, the expression of clock genes and the induction of *PER1* expression by Dex and Frk stimulation were not enhanced by EZH2 inhibition alone in 201B7 iPSCs (Fig. 2A, B). This phenomenon may also result from unchanged H3K27ac modification in their promoter. In the presence of TSA treatment, GSK126 significantly increased *PER1*, *PER2*, and *BMAL1* expression (Suppl. Fig. S10). Furthermore, transcription factors, such as glucocorticoid receptor and CREB activated by Dex and Frk, respectively, could not be recruited to promoters with GSK126 treatment alone because of insufficient active mark H3K27ac. When H3K27ac modifications increased in the TSS, the chromatin structure would become accessible for the binding of stimulus-dependent transcription factors [36].

Previous reports have studied the expression level of BMAL1 in PSCs and its difference with another cell types. Ameneiro et al. analyzed *BMAL1* mRNA and protein levels and found that these levels were higher in mouse ESCs than in mouse embryonic fibroblasts [37]. In addition, Gallardo et al. compared *BMAL1* mRNA and protein levels between

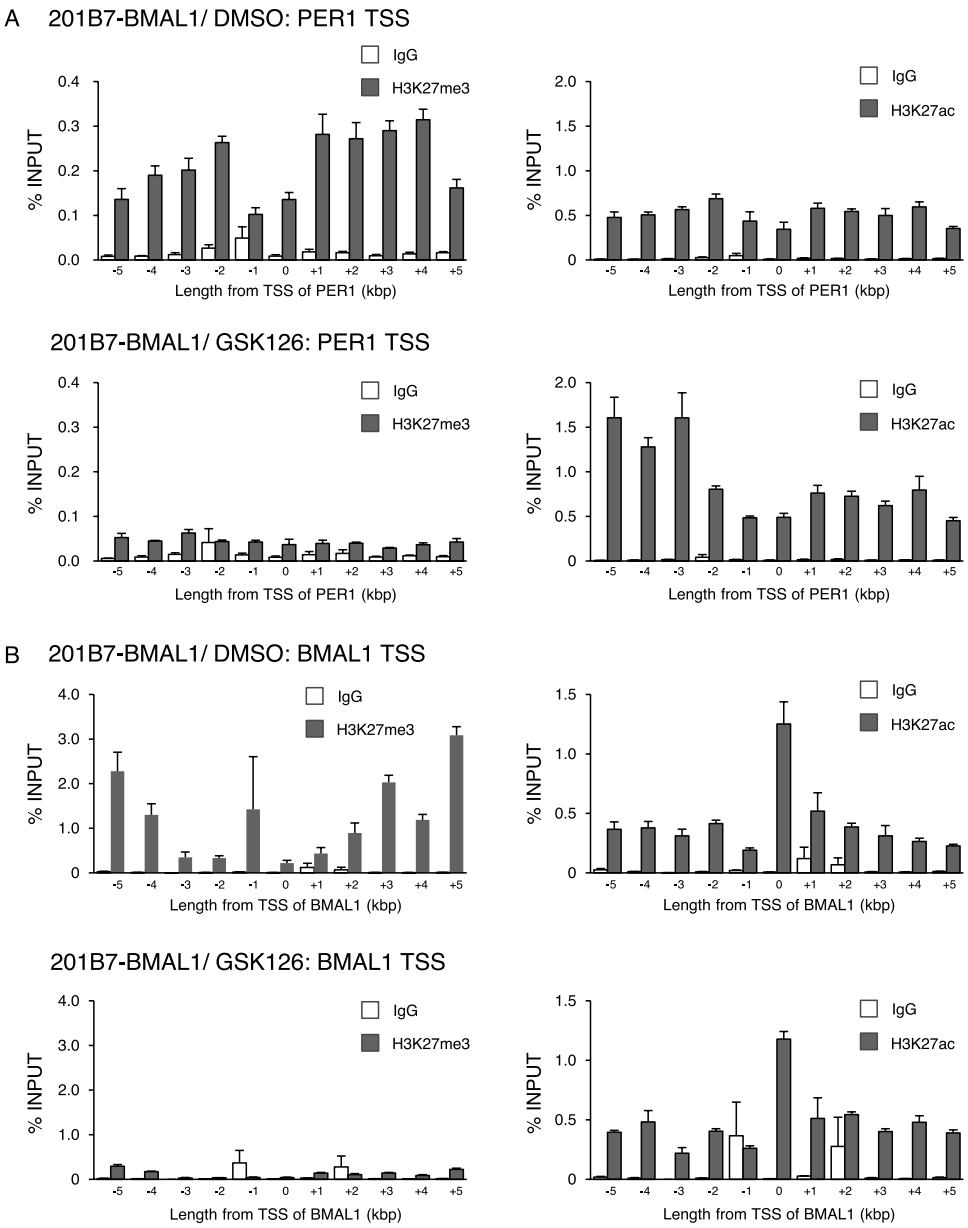

Fig. 6 Effect of GSK126 treatment on H3K27 modification levels in the TSS of *PER1* in iPSC-BMAL1 cells. **A, B** ChIP-qPCR analysis of H3K27 me3 and H3K27ac. The percentage of each precipitated DNA fragment around the TSS of *PER1* (**A**) and *BMAL1* (**B**) by anti-H3K27 me3 and H3K27ac antibodies to INPUT was analyzed in 201B7-BMAL1 cells treated with DMSO or 5 μM GSK126 for 48 h. The 0 on the *x*-axis indicates the 200-bp region around the TSS. + 1 to + 5 and − 1 to − 5 on the *x*-axis indicates the 200-bp region around 1–5 kbp upstream or downstream of the TSS, respectively. Next, data are presented as means ± SEM; $n = 3$ for independent experiments for each comparison

mouse ESCs and its differentiated NSCs and found that these cells expressed similar levels, indicating that BMAL1 is expressed at functional levels in mouse ESCs [38]. With regard to human PSCs, Thakur et al. showed that *BMAL1* mRNA is expressed in human ESCs, and its level was unchanged under spontaneous differentiation [39]. These findings are inconsistent with the results obtained from our present and previous studies [16]. In another report, Dierickx et al. examined the expression level of clock genes between human ESCs and U2OS cells and found that all genes were detected in both cell types. Among them, five clock genes, including *BMAL1*, had lower levels in human ESCs compared with U2OS cells [2]. This finding is consistent with our results. Therefore, human iPSCs express BMAL1, whereas its level is lower than that of U2OS cells, which possess a functional clock, indicating that such levels of BMAL1 might be not enough for maintaining the circadian clock. As shown in Fig. 3, BMAL1 overexpression significantly increased the expression of most clock genes in iPSCs. BMAL1 heterodimerizes with CLOCK to recognize E-box motifs and regulate the expression of thousands of genes, which is referred to as clock-controlled genes [40]. *PER1*, *PER2*, *PER3*, *CRY1*, *CRY2*, *DBP*, *NR1D1*, and *NR1D2* contain E-boxes in their promoters, and their expression is directly regulated by CLOCK/BMAL1 [7]. However, the expression level of *RORA* and *RORB* was not increased by BMAL1 overexpression probably because these genes do not contain an E-box in their promoter regions. Therefore,

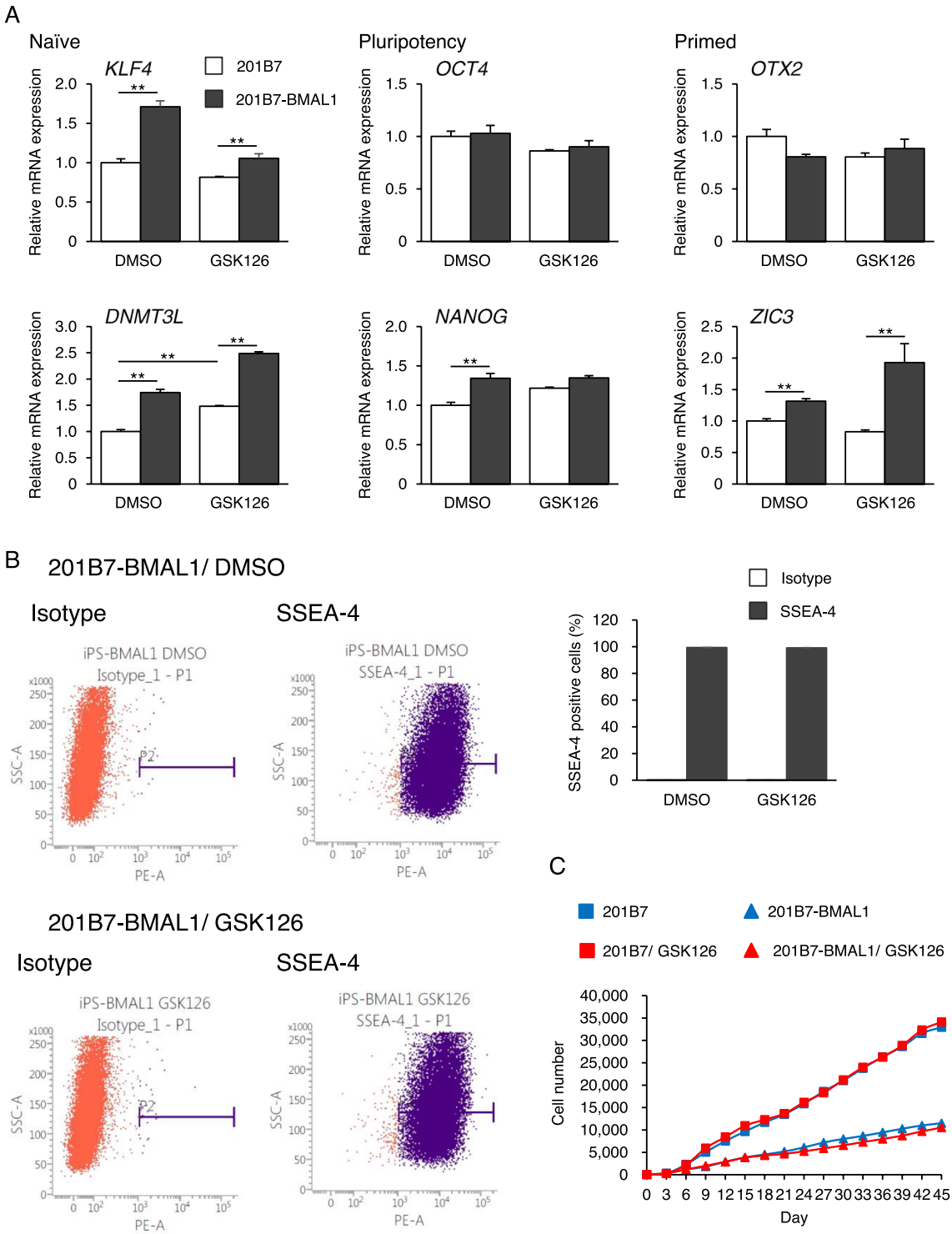

Fig. 7 Effect of BMAL1 overexpression and GSK126 treatment on pluripotency in iPSCs. **A** Expression levels of naïve, pluripotency, and primed marker genes were measured in 201B7 iPSCs and 201B7-BMAL1 cells treated with or without 5 μM GSK126 for 48 h. Next, data are presented as means ± SEM relative to DMSO-treated 201B7 iPSCs; $n = 6$ for independent experiments for each comparison. **B** The percentage of SSEA-4-positive cells was analyzed in 201B7-BMAL1 after treatment with DMSO or 5 μM GSK126 for 48 h by FACS. P2 indicates the range of SSEA-4-positive cells, and the bar graph shows the percentage of SSEA-4-positive cells for each treatment. Data are presented as means ± SEM; $n = 3$ for each comparison. **C** Growth curve was evaluated in 201B7 iPSCs and 201B7-BMAL1 cells treated with or without 5 μM GSK126 throughout the culture

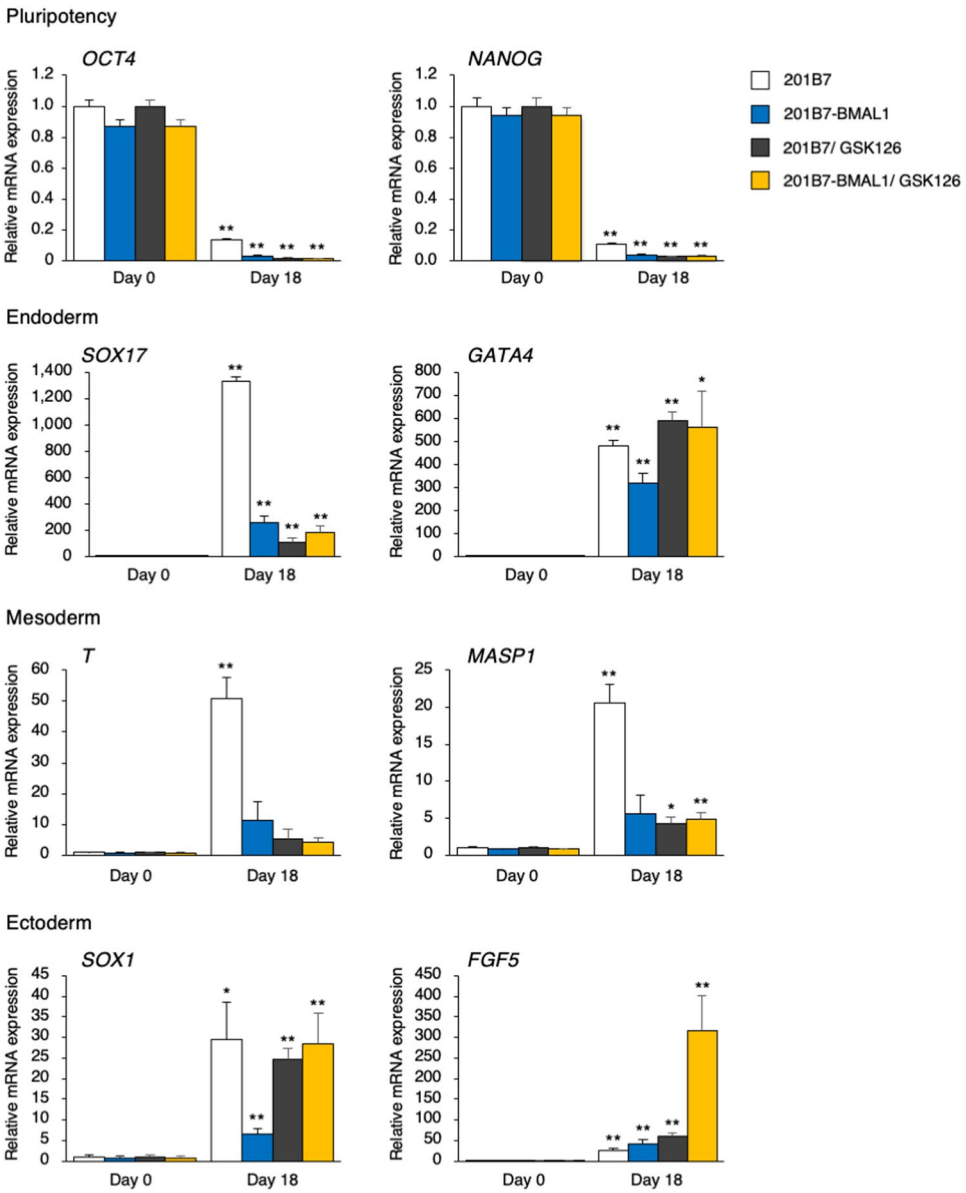

Fig. 8 Effect of BMAL1 overexpression and GSK126 treatment on differentiation capacity in iPSCs. **A** iPSCs were cultured in non-adherent dishes for the formation of embryoid bodies (EBs). After 18 days of EB formation, the expression level of pluripotency, endoderm, mesoderm, and ectoderm marker genes was measured in 201B7 iPSCs and 201B7-BMAL1 cells pretreated with or without 5 μM GSK126 for 48 h before EB formation. Next, data are presented as means ± SEM relative to DMSO-treated 201B7 iPSCs at day 0 before EB formation; $n = 4$ for independent experiments for each comparison. $^{*}P < 0.05$, $^{**}P < 0.01$ versus each value of corresponding control at day 0

exogenous BMAL1 expression induces clock genes that contain E-boxes. With regard to CLOCK protein, detectable levels were observed in several iPSC lines by Western blot analysis (Suppl. Fig. S11B). Umemura et al. showed that CLOCK protein is post-transcriptionally repressed and gradually emerged during development in mouse and human PSCs [13], whereas Dierickx et al. detected CLOCK protein in human ESCs [2]. Further studies, including functional analysis on CLOCK protein in PSCs with somatic cells, are necessary for final conclusion.

The combination of BMAL1 overexpression and EZH2 inhibition induces the circadian oscillation of *PER2* and endogenous expression of *BMAL1*, *CRY1*, and *PER1* in iPSCs (Fig. 5, Suppl. Fig. S12). This phenomenon occurs because exogenous BMAL1 markedly increases clock gene expression, which functions in the circadian feedback loop. GSK126 treatment removes repressive epigenetic modifications of histone such as H3K27 me3 and causes iPSCs to become sensitive and responsive to synchronizing agents, which is supported by the increase of active markers such as H3K27ac in the TSS of *PER1* (Fig. 6). Theoretically, Dex and Frk stimulations transiently induce *PER1* and subsequently the expression of *PER2* and *DBP*, which are synchronized and oscillated for 24 h in mammalian cells [41, 42]. Similarly, these two agents worked to synchronize the circadian rhythm in iPSCs with BMAL1 and GSK126. However, different results were obtained between Dex and Frk stimulation. Dex stimulation induced significant rhythms of *PER2* and endogenous *BMAL1* expression, whereas Frk induced only the *PER2* rhythm (Fig. 5A, B). This result

could be due to the differences in responsiveness to Dex and Frk stimulation among cell types as expected from our previous study, in which the activation of transcription factor is different among iPSCs, U2OS, and BJ cells [16]. At 48 h, the rhythms of *PER2*, *CRY1*, and *PER1* expressions after Dex stimulation were significant compared with endogenous *BMAL1* and *CLOCK* in 201B7 iPSCs, indicating that this artificial induction of the circadian rhythm is not fully achieved (Suppl. Fig. S12A). The overexpression of CLOCK protein or dual inhibition of EZH1 and EZH2 could be applied for the complete development of the circadian rhythm in iPSCs. In addition to the response to synchronizing agents, differences in the rhythmicity of clock genes were observed between the iPSC lines 201B7 and 1383D6. 1383D6 iPSCs showed the significant rhythm of *PER2* expression with BMAL1 overexpression alone (Suppl. Fig. S12A), indicating that EZH2 inhibition is not essential for the rhythmicity of some clock genes in this cell line. Supporting this idea, the levels of H3K27 me3 around the *PER2* TSS were naturally lower in 1383D6 iPSCs compared with 201B7 (Suppl. Figs. S6A and S9A). These differences could be due to the gender of their origins. Theoretically, male and female iPSCs display differential enrichment of epigenetic marks including PRC2-mediated H3K27 me3 modification in some genes on not only sex chromosomes but also autosomes [22]. This phenomenon might lead to sex differences in the regulation of clock gene expression and response to synchronizing stimulation between male and female iPSCs. iPSCs with BMAL1 overexpression and GSK126 treatment normally express the pluripotency marker genes and SSEA-4, whereas the proliferation rate is reduced by BMAL1 overexpression (Fig. 8C). It is suggested that regulatory pathway of cell cycle could be affected by BMAL1 overexpression because the proportion of apoptotic cells was unchanged during proliferation (Suppl. Figure 13C). Clock genes and circadian rhythm are linked to cell cycle system and some studies have shown that disrupted circadian rhythm is related to cancer cell proliferation [43–45]. Exogenous CLOCK expression restores disrupted circadian oscillation in murine breast cancer 4T1 cells and reduces their growth ability [45]. Therefore, the induction of the circadian rhythm by exogenous clock proteins could affect the proliferation capacity in cells with defective circadian clock machinery. However, significant rhythms of any clock genes were not detected in BMAL1-overexpressing 201B7 iPSCs without GSK126 treatment. Therefore, it is unclear yet whether induced circadian rhythm leads to a reduction of proliferation or reduced proliferation promotes an induction of circadian rhythm in iPSCs. Further examinations must be performed to elucidate the relationship between the absence of circadian rhythm and proliferation ability in PSCs. With regard to the differentiation capacity, iPSCs with the abovementioned treatments showed a different tendency to differentiate into three germ layers compared with intact iPSCs, showing that BMAL1 overexpression or EZH2 inhibition could have some effects on the differentiation program. Whether whole body organs are normally developed from iPSCs expressing intact circadian clock machinery remains to be determined. Therefore, pup generation from mouse iPSCs must be examined by artificial induction of circadian rhythm in future studies to address the abovementioned question.

Next, the function of clock genes and the circadian rhythm during mammalian embryonic development are not fully understood. In rodents and primates, clock genes are expressed in oocytes and during early and late development in embryo/fetal organs [46, 47]. Umemura et al. showed that the oscillation of a cell-autonomous molecular clock was not detected around embryonic day 10, whereas oscillation was observed just before birth at embryonic day 18 [13]. Any mouse lacking Bmal1, Clock, Cry1, Cry2, Per1, and Per2 is normally born with no apparent phenotype at birth, which indicates that these genes and their oscillation are not essential for organ development [17, 48–51]. By contrast, recent studies have supported the role of clock genes in organ development. Gallard et al. showed that Bmal1 knockout mouse ESCs exhibit deficient multi-lineage cell differentiation capacity [38]. Moreover, Ameneiro et al. demonstrated that the depletion of BMAL1 results in the deregulation of transcriptional programs linked to cell differentiation commitment and disrupted gastrulation in vitro, although BMAL1 was dispensable for the maintenance of the pluripotent state in mouse ESCs [37].

With regard to the role of BMAL1 in the expression of pluripotency genes of human PSCs, *NANOG* mRNA levels were significantly higher in BMAL1-overexpressing iPSCs (Fig. 7A). However, Gallardo et al. reported that mRNA and protein levels of Nanog significantly increased Bmal1 knockout ESCs, whereas Amneiro et al. showed that those levels were not significantly affected in Bmal1 knockout ESCs. This discrepancy could be due to the differences in primed and naïve state of human and mouse PSCs, respectively. Therefore, the effect of BMAL1 overexpression or deletion on NANOG expression should be tested in naïve human PSCs. In addition, this study provided a new insights into the effect of BMAL1 on the expression of naïve and primed marker genes in iPSCs. BMAL1 overexpression increased the naïve markers *KLF4* and *DNMT3L* (Fig. 7A). This finding suggests that BMAL1 could play a role in the transition from primed to naïve state of human PSCs because KLF4 is a key factor affecting the conversion of human PSCs into naïve pluripotent state and their maintenance [52, 53].

Finally, this study shows a possible link between clock gene regulation and proliferation ability in infinitely growing cells, providing a therapeutic strategy for inhibiting the proliferation of such cells, such as cancer cells. Furthermore, this study provides an experimental tool for investigating the

role of circadian rhythm in developing and establishing differentiation methods through circadian oscillation.

Materials and methods

Cell culture

The iPSC line, including 201B7 [26], 1383D6, 1231A3, and 585A1 [54], was obtained from Riken BRC and maintained in the Cellartis® DEF-CS™ 500 culture system (Takara bio) under feeder-free conditions at 37 °C and 5% CO_2 according to the manufacturer's instructions. Next, U2OS cells were obtained from the ATCC. HDF was obtained from Cell Applications, Inc. TIG-114 and TIG-120 were obtained from the Japanese Collection of Research Bioresources, and BJ was obtained from the ATCC. Then, U2OS, HDF, TIG-114, TIG-120, and BJ cells were cultured in 10% fetal bovine serum (FBS, Merck) containing 100 units/mL of penicillin and 0.1 mg/mL of streptomycin (Thermofisher Scientific) in high-glucose Dulbecco's modified Eagle medium (DMEM, Thermofisher Scientific) at 37 °C and 5% CO_2.

Establishment of the BMAL1-expressing cell line

The BMAL1 coding sequence was inserted into the multiple cloning site of the pLVSIN-EF1α Pur Vector (Takara bio) and transfected into HEK293FT cells. After 48 h, the viral supernatant was collected and filtered. After infecting iPSCs with the virus, the cells were added with 0.2 μg/mL of puromycin for 2 weeks to establish the BMAL1-expressing iPSC line.

Quantitative real-time PCR (qPCR)

Total RNA was extracted from cells using TRIzol reagent (Thermofisher Scientific) according to the manufacturer's instructions. cDNA synthesis was performed using the SuperScript VILO cDNA Synthesis Kit (Thermofisher Scientific). qPCR was performed using the ViiA7 Real-Time PCR System with PowerUp SYBR Green Master Mix (Thermofisher Scientific). Gene expression was normalized to the expression of *18S*. Primer sequences are shown in Table 1. For the GSK126-treated group, RNA was extracted 48 h after 5 μM GSK126 was added to the culture medium. The

Table 1 Sequence of primers used for qPCR

Gene	Forward	Reverse
18S	GAGGATGAGGTGGAACGTGT	GGACCTGGCTGTATTTTCCA
DBP	CCAATCATGAAGAAGGCAAGAAA	GGCTGCCTCGTTGTTCTTGT
BMAL1 (CDS)	GAGAAGGTGGCCCAAAGAGG	GGAGGCGTACTCGTGATGTT
CLOCK	ACGACGAGAACTTGGCATTG	TCCGAGAAGAGGCAGAAGG
PER1	CCCAGCACCACTAAGCGTAAA	TGCTGACGGCGGATCTTT
PER2	GCTGGCCATCCACAAAAAGA	GCGAAACCGAATGGGAGAAT
PER3	GCCTTACAAGCTGGTTTGCAA	CTGTGTCTATGGACCGTCCATTT
CRY1	ACTCCCGTCTGTTTGTGATTCG	GCTGCGTCTCGTTCCTTTCC
CRY2	TCTTCCAGCAGTTCTTCC	GTAGTCCACACCAATGATG
NR1D1	CTGCAGGGTGCTTCGGA	GCCAATGTAGGTGATGACGC
NR1D2	GAGTGCACCTGGGATGACAA	TACAGCCTTCGCAAGCATGA
RORA	GAGCCAGGCAGCAGCG	GTCTCCACAGATCTTGCATGG
RORB	AGGGATGGTTTTCTCGGCAG	CCCAGAGGACTTATCGCCAC
BMAL1 (3'UTR)	ACAAAGTGGAACTAAGCCTGC	AAGCTACCAATGATGCTTCTG
BMAL1 (FLAG)	ATGGACTACAAAGACGATGAC	TGGTACCAAGAGAGCTGGAA
KLF4	GACAGTGGATATGACCCACACTGCC	GATAGAAGATCCAGTCACAGACC
DNMT3L	ATGAAGTCAAGGCTAACCAGC	CGTCATCGTCGTACAGGAAGAG
OCT4	AGTTTGTGCCAGGGTTTTTG	ACTTCACCTTCCCTCCAACC
NANOG	TACCTCAGCCTCCAGCAGAT	TGCGTCACACCATTGCTATT
OTX2	CAAAGTGAGACCTGCCAAAAAGA	TGGACAAGGGATCTGACAGTG
ZIC3	CGGCGCACGATCTATCTTCAG	TGGCGGAACAGAAACTCGC
SOX17	GCATGACTCCGGTGTGAATCT	TCACACGTCAGGATAGTTGCAGT
GATA4	CCTGTCATCTCACTACGG	GCTGTTCCAAGAGTCCTG
T	ATGACAATTGGTCCAGCCTTGG	TACTGGCTGTCCACGATGTCTG
MESP1	ACCTTGGAAGTGGTTCCTTG	TCCTGCTTGCCTCAAAGTGT
SOX1	ATGCACCGCTACGACATGG	CTCATGTAGCCCTGCGAGTTG
FGF5	ACGAGGAGTTTTCAGCAACAAAT	TTGGCACTTGCATGGAGTTTT

control, DMSO-treated group was added with the culture medium at a concentration of 0.1%. In addition, for the Dex or Frk stimulation group, 0.1 μM Dex or 10 μM Frk was added to the culture medium after 48 h of pre-treatment with DMSO or GSK126, and RNA was extracted after 0, 60, and 120 min. In the TSA-treated group, 0.1 μM TSA was added to the culture medium after 48 h of pre-treatment with 0.1% DMSO or 5 μM GSK126, and RNA was extracted after 24 h.

Western blot analysis

Cells were lysed using RIPA buffer (50 mM Tris–HCl, pH 8.0, 150 mM NaCl, 1% NP-40, 0.5% sodium deoxy cholate, 0.5% SDS, and 1% protease inhibitor cocktail) and sonicated. Then, the lysates were cleared by centrifugation at 15,000*g* for 20 min, and Laemmli's sample buffer (0.38 M Tris–HCl, pH 6.8, 12% SDS, 30% β-mercaptoethanol, 10% glycerol, and 0.05% bromophenol blue) was added to the supernatant. The samples were boiled at 95 °C for 5 min, and each 30 μg as total protein was subjected to SDS-PAGE, then transferred to polyvinylidene difluoride membranes. The transferred membranes were blocked with Blocking One (Nacalai Tesque) and incubated with anti-BMAL1 (14020, Cell Signaling Technologies), anti-CLOCK (ab3517, Abcam), anti-tri-methyl-histone H3K27 (9733, Cell signaling technologies), anti-β-actin (M177-3, Medical and Biological Laboratories), or anti-histone H3 (4499, Cell Signaling Technologies) antibodies at 4 °C overnight. Next, the membranes were washed and incubated with horseradish peroxidase-conjugated anti-rabbit IgG (Thermofisher Scientific) or anti-mouse IgG (Dako) for 1 h. Then, the membranes were washed and incubated with Amersham™ ECL™ Prime Western Blotting Detection Reagent (Cytiba). For imaging of the membrane, proteins were measured using an ImageQuart 400 instrument (Cytiba) and quantified using ImageJ. The levels of β-actin or total histone H3 were used as normalization controls in each corresponding experiment.

ChIP-qPCR

ChIP assays were performed using a SimpleChIP® Plus Enzymatic Chromatin IP Kit (Cell Signaling Technologies) according to the manufacturer's instructions. For immunoprecipitation, anti-tri-methyl-histone H3K27 and anti-acetyl-histone H3K27 antibodies (8173, Cell Signaling Technologies) were used. For the GSK126-treated group, each cell was stimulated with 5 μM GSK126 for 48 h, and then it was fixed with formaldehyde and harvested. DNA fragments from the ChIP assay were quantified by qPCR using primers that amplify 200 bp around the TSS of *PER1*, *BMAL1*, or *PER2*. The primer sequences are shown in Table 2.

Stimulation to synchronize the circadian rhythm

For synchronization of circadian rhythms, Dex or Frk was used. For Dex stimulation, the cells were stimulated for 2 h in a culture medium containing 0.1 μM Dex, which was then changed to a culture medium without Dex, and RNA was collected every 4 h. For Frk stimulation, the cells were stimulated for 1 h in a culture medium containing 10 μM Frk, and then they were changed to a culture medium without Frk. RNA was collected every 4 h. The extracted RNA was reverse-transcribed, and the expression of *PER2*, *BMAL1 CLOCK*, *CRY1*, and *PER1* was measured by qPCR analysis.

Flow cytometry

Cells were harvested with TrypLE Select (Thermofisher Scientific) and washed with 1% bovine serum albumin (BSA)-PBS. The cells were resuspended in 1% BSA-PBS containing anti-human SSEA-4 (12-8843-41, Thermofisher Scientific) or anti-mouse IgG3 isotype control (Thermofisher Scientific) and incubated on ice for 45 min. The cells were washed and resuspended in 1% BSA–PBS. The number of SSEA-4-positive cells was analyzed using a FACSVerse flow cytometer (BD). For the detection of apoptosis, annexin V was labeled with FITC conjugated reagent and DNA was stained with propidium iodide (PI) according to the manufacturer's instructions using the Annexin V-FITC Apoptosis Detection Kit (Nacalai Tesque). Then, detection was performed by FACSVerse flow cytometer. Flow cytometer data were analyzed using FACSuite (BD).

Cell proliferation assay

6×10^5 cells were seeded and cultured for 3 days, and then the cell number was counted. Cells were passaged every 3 days, and this process was repeated 15 times. The cumulative cell number was calculated on the basis of the number of cells. The GSK126-treated group was always maintained in a medium with 5 μM GSK126.

Immunocytochemistry

Cells were washed with PBS and fixed in 4% paraformaldehyde (FUJIFILM Wako) for 30 min. The samples were permeabilized with 0.1% Triton X-100 (Nacalai Tesque) for 15 min. Blocking was performed with Blocking One for 10 min. The primary antibody reaction was performed using an anti-Oct4 antibody (sc-5279, Santa Cruz Biotechnology) at 4 °C overnight. Cells were washed with PBS and incubated with an Alexa Fluor 568-conjugated secondary antibody (Thermofisher Scientific), followed by incubation with DAPI (Merck) for 1 h. Images were taken by using an Olympus FV3000 microscope (Olympus Optical Co. Ltd.).

Table 2 Sequence of primers used for ChIP-qPCR

Genomic region	Forward	Reverse
PER1 TSS − 5	GCCCCCTTTCTCCTGTTGAC	TTCATATTTCCACTGCTTGG
PER1 TSS − 4	GCCCTTGCCACCCCACATTT	CTTCTATGGCCACTCAGAGA
PER1 TSS − 3	CACCTGCCATTGTTTCCCTT	CCCAACCTTGTTCCCTCCCA
PER1 TSS − 2	AAAGGAACCCAGGAGAGGCC	CCCGGCCCGGGGTAGGTGCT
PER1 TSS − 1	CTTTTTCCCTAAAGAGGCGC	TCTCTTCCCGGCGCCTGATT
PER1 TSS 0	AGAGATCCCCAGCCAATCGG	CGGAGATCGGCCCCAGGATG
PER1 TSS + 1	CTCCGTCCCTGAGCCGGACC	GGGACGGGGAGGTGGGGACA
PER1 TSS + 2	AGCTTTCCCGGCCCCACAGC	AGCGCTGGGAACGGGATGTT
PER1 TSS + 3	GGTTCCTGCTGTTGGCCACA	CGTCAAGGACCCGAGGATCC
PER1 TSS + 4	ATGGCAGGTTGCCGGCTTCG	GTGGGACGGCCTATTAGGAT
PER1 TSS + 5	TTCTTACGGCCACCGAGCCA	ACGGTCGCCAGGGAAACCGA
BMAL1 TSS − 5	GAAAAAGAAGACGCTGTCCT	GCTGTCTACGGAGCAAGACG
BMAL1 TSS − 4	TTTTTGCAGCAGAGAGCGCT	CCCCGAGGACTGCAAGTGTT
BMAL1 TSS − 3	TGGAAATGCCTTCTAGAAAT	CGCCCTCACCCCTCCTCCTT
BMAL1 TSS − 2	GGCGGCCAAACGCCAGCCGG	AATCATTTGGCGCACAGGAG
BMAL1 TSS − 1	GGTGGCAGGAAAGTAGCAGG	ATGGAGGAGCCGCAGCGCCC
BMAL1 TSS 0	TGGTGGGCGGGGAAGGGGGG	CGCGCCCGCACTCGGATCCC
BMAL1 TSS + 1	GGCGCGGGCGCTCCCGGCGA	GCAGGGAGCGGTCACGGGCC
BMAL1 TSS + 2	CCCCACCCGGGCCGTGGGGA	TAGCTGCCCCCTCCCCCCGC
BMAL1 TSS + 3	GCTGCCTCTTAAAGGGATAG	CACCCAGCCTCGCGGGCTCC
BMAL1 TSS + 4	GGGGCGGGGAGGGCGTCTCC	CGCACCTGCCCGCAGACCCA
BMAL1 TSS + 5	CGTCGGCCTGGGGATGTCGC	CTCTACCTTCCTCGTCTTCT
PER2 TSS − 3	GAGTGAGTGAATGAGTAAAT	CGGGCGGGGGAGCTGG
PER2 TSS − 2	CAATGGTACGCGCCACTCCG	GGCCGCGCCCGTCGCTCTTT
PER2 TSS − 1	ACCAATGGGCGCGCGGCGTT	CCCGCGCCCGCCGCCGCCGC
PER2 TSS 0	GCCGGGCGGACAGAGCCGCG	GGAGTCCAGCAGCCCAAGGA
PER2 TSS + 1	TCGGCTTGAAACGGCGCCGG	TCACTCGGTAGCTCGGTGCC
PER2 TSS + 2	CTGCGCGCGGGCTGCGGTTC	TCCTAGATCAGCGCCCCTCC
PER2 TSS + 3	GCTTTTCCTGGACACCCACG	CTGCACCAAAGAGTGGACAC

Embryoid bodies formation assay

201B7 was seeded in DMEM/F12 (Thermo Fisher Scientific) with 20% Knockout Serum Replacement (Thermo Fisher Scientific), 2 mM L-glutamine (Thermo Fisher Scientific), 0.1 mM NEAA (Thermo Fisher Scientific), 0.1 mM 2-mercaptoethanol (Merck), and 10 µM Y-27632 (Nacalai Tesque) at 9000 cells/well in a low-attachment surface V-bottom 96-well plate (Sumitomo Bakelite). The culture medium was changed every 2 days for 11 days, and then cells were cultured in DMEM with 10% FBS on 0.1% gelatin-coated culture plates for 7 days, with medium changed every 2 days. Then, RNA was extracted, and qPCR was performed.

Statistical analyses

Data in all graphs were expressed as the mean ± standard error of the mean (SEM). Comparisons between two groups shown in Figs. 2A, 4B, 7B, and 8 were analyzed by using two-tailed asymmetric Student's *t*-test. For multiple comparisons, one-way analysis of variance followed by Dunnet's post-hoc analysis was performed in Figs. 2B, 3B, C, 4A, 7A. For significant rhythm determination in Fig. 5A, B, cosinor analysis was performed for all 24-h time series. *P*-values less than 0.05 were considered statistically significant.

Supplementary Information The online version contains supplementary material available at https://doi.org/10.1007/s00018-023-04847-z.

Acknowledgements This research was funded by Japan Society for the Promotion of Science, grant number KAKENHI 18K06876, and Adaptable and Seamless Technology transfer Program through Target-driven R&D (A-STEP) from Japan Science and Technology Agency Grant Number JPMJTM19GL. The authors would like to thank Enago (www.enago.jp) for the English language review.

Author contributions HK performed experiments. HK, TK, and KT designed experiments and analyzed data. HK and TK wrote the paper. TK and KT oversaw the project.

Funding This work was supported by Japan Society for the Promotion of Science (JSPS) KAKENHI Grant Number JP18K06876 and by Adaptable and Seamless Technology transfer Program through Target-driven R&D (A-STEP) from Japan Science and Technology Agency Grant Number JPMJTM19GL.

Availability of data The datasets generated during and/or analyzed during the current study are available from the corresponding author on reasonable request.

Declarations

Conflict of interest The authors declare no competing interests.

Ethics approval and consent to participate Not applicable.

Consent for publication Not applicable.

References

1. Umemura Y, Maki I, Tsuchiya Y et al (2019) Human circadian molecular oscillation development using induced pluripotent stem cells. J Biol Rhythms 34:525–532. https://doi.org/10.1177/0748730419865436
2. Dierickx P, Vermunt MW, Muraro MJ et al (2017) Circadian networks in human embryonic stem cell-derived cardiomyocytes. EMBO Rep 18:1199–1212. https://doi.org/10.15252/embr.201743897
3. Vilchez D, Boyer L, Morantte I et al (2012) Increased proteasome activity in human embryonic stem cells is regulated by PSMD11. Nature 489:304–308. https://doi.org/10.1038/nature11468
4. Lee HJ, Gutierrez-Garcia R, Vilchez D (2017) Embryonic stem cells: a novel paradigm to study proteostasis? FEBS J 284:391–398. https://doi.org/10.1111/febs.13810
5. Banito A, Gil J (2010) Induced pluripotent stem cells and senescence: learning the biology to improve the technology. EMBO Rep 11:353–359. https://doi.org/10.1038/embor.2010.47
6. Sancar G, Brunner M (2014) Circadian clocks and energy metabolism. Cell Mol Life Sci 71:2667–2680. https://doi.org/10.1007/s00018-014-1574-7
7. Takahashi JS (2017) Transcriptional architecture of the mammalian circadian clock. Nat Rev Genet 18:164–179. https://doi.org/10.1038/nrg.2016.150
8. Papazyan R, Zhang Y, Lazar MA (2016) Genetic and epigenomic mechanisms of mammalian circadian transcription. Nat Struct Mol Biol 23:1045–1052. https://doi.org/10.1038/nsmb.3324
9. Saini C, Morf J, Stratmann M et al (2012) Simulated body temperature rhythms reveal the phase-shifting behavior and plasticity of mammalian circadian oscillators. Genes Dev 26:567–580. https://doi.org/10.1101/gad.183251.111
10. Paulose JK, Rucker EB, Cassone VM (2012) Toward the Beginning of time: circadian rhythms in metabolism precede rhythms in clock gene expression in mouse embryonic stem cells. PLoS ONE 7:e49555. https://doi.org/10.1371/journal.pone.0049555
11. Yagita K, Horie K, Koinuma S et al (2010) Development of the circadian oscillator during differentiation of mouse embryonic stem cells in vitro. Proc Natl Acad Sci USA 107:3846–3851. https://doi.org/10.1073/pnas.0913256107
12. Umemura Y, Koike N, Matsumoto T et al (2014) Transcriptional program of Kpna2/Importin-α2 regulates cellular differentiation-coupled circadian clock development in mammalian cells. Proc Natl Acad Sci USA 111:E5039–E5048. https://doi.org/10.1073/pnas.1419272111
13. Umemura Y, Koike N, Ohashi M et al (2017) Involvement of posttranscriptional regulation of *Clock* in the emergence of circadian clock oscillation during mouse development. Proc Natl Acad Sci USA 114:E7479–E7488. https://doi.org/10.1073/pnas.1703170114
14. Li M, Liu G-H, Belmonte JCI (2012) Navigating the epigenetic landscape of pluripotent stem cells. Nat Rev Mol Cell Biol 13:524–535. https://doi.org/10.1038/nrm3393
15. Guenther MG, Frampton GM, Soldner F et al (2010) Chromatin structure and gene expression programs of human embryonic and induced pluripotent stem cells. Cell Stem Cell 7:249–257. https://doi.org/10.1016/j.stem.2010.06.015
16. Kaneko H, Kaitsuka T, Tomizawa K (2020) Response to stimulations inducing circadian rhythm in human induced pluripotent stem cells. Cells 9:620. https://doi.org/10.3390/cells9030620
17. Bunger MK, Wilsbacher LD, Moran SM et al (2000) Mop3 is an essential component of the master circadian pacemaker in mammals. Cell 103:1009–1017. https://doi.org/10.1016/S0092-8674(00)00205-1
18. Stratmann M, Suter DM, Molina N et al (2012) Circadian Dbp transcription relies on highly dynamic BMAL1-CLOCK interaction with E boxes and requires the proteasome. Mol Cell 48:277–287. https://doi.org/10.1016/j.molcel.2012.08.012
19. Chan HL, Beckedorff F, Zhang Y et al (2018) Polycomb complexes associate with enhancers and promote oncogenic transcriptional programs in cancer through multiple mechanisms. Nat Commun 9:3377. https://doi.org/10.1038/s41467-018-05728-x
20. Schuettengruber B, Bourbon H-M, Di Croce L, Cavalli G (2017) Genome regulation by polycomb and trithorax: 70 years and counting. Cell 171:34–57. https://doi.org/10.1016/j.cell.2017.08.002
21. Atlasi Y, Stunnenberg HG (2017) The interplay of epigenetic marks during stem cell differentiation and development. Nat Rev Genet 18:643–658. https://doi.org/10.1038/nrg.2017.57
22. Yokobayashi S, Yabuta Y, Nakagawa M et al (2021) Inherent genomic properties underlie the epigenomic heterogeneity of human induced pluripotent stem cells. Cell Rep 37:109909. https://doi.org/10.1016/j.celrep.2021.109909
23. Yan P, Liu Z, Song M, Belmonte JCI, Xie W, Ren J, Zhang W, Sun Q, Qu J, Liu GH (2020) Genome-wide R-loop landscapes during Cell differentiation and reprogramming. Cell Rep 32:107870. https://doi.org/10.1016/j.celrep.2020.107870
24. Vollmers C, Panda S, DiTacchio L (2008) A high-throughput assay for siRNA-based circadian screens in human U2OS cells. PLoS One 3:e3457. https://doi.org/10.1371/journal.pone.0003457
25. McCabe MT, Ott HM, Ganji G et al (2012) EZH2 inhibition as a therapeutic strategy for lymphoma with EZH2-activating mutations. Nature 492:108–112. https://doi.org/10.1038/nature11606
26. Takahashi K, Tanabe K, Ohnuki M et al (2007) Induction of pluripotent stem cells from adult human fibroblasts by defined factors. Cell 131:861–872. https://doi.org/10.1016/j.cell.2007.11.019
27. Nakagawa M, Taniguchi Y, Senda S et al (2014) A novel efficient feeder-free culture system for the derivation of human induced pluripotent stem cells. Sci Rep 4:3594. https://doi.org/10.1038/srep03594
28. Chin MH, Mason MJ, Xie W et al (2009) Induced pluripotent stem cells and embryonic stem cells are distinguished by gene expression signatures. Cell Stem Cell 5:111–123. https://doi.org/10.1016/j.stem.2009.06.008
29. Bernstein BE, Mikkelsen TS, Xie X et al (2006) A bivalent chromatin structure marks key developmental genes in embryonic stem cells. Cell 125:315–326. https://doi.org/10.1016/j.cell.2006.02.041
30. Margueron R, Reinberg D (2011) The Polycomb complex PRC2 and its mark in life. Nature 469:343–349. https://doi.org/10.1038/nature09784

31. Pan G, Tian S, Nie J et al (2007) Whole-genome analysis of histone H3 lysine 4 and lysine 27 methylation in human embryonic stem cells. Cell Stem Cell 1:299–312. https://doi.org/10.1016/j.stem.2007.08.003
32. Harikumar A, Meshorer E (2015) Chromatin remodeling and bivalent histone modifications in embryonic stem cells. EMBO Rep 16:1609–1619. https://doi.org/10.15252/embr.201541011
33. Etchegaray J-P, Yang X, DeBruyne JP et al (2006) The polycomb group protein EZH2 is required for mammalian circadian clock function. J Biol Chem 281:21209–21215. https://doi.org/10.1074/jbc.M603722200
34. Margueron R, Li G, Sarma K et al (2008) Ezh1 and Ezh2 maintain repressive chromatin through different mechanisms. Mol Cell 32:503–518. https://doi.org/10.1016/j.molcel.2008.11.004
35. Lee SH, Li Y, Kim H et al (2022) The role of EZH1 and EZH2 in development and cancer. BMB Rep 55:595–601. https://doi.org/10.5483/BMBRep.2022.55.12.174
36. Mayran A, Drouin J (2018) Pioneer transcription factors shape the epigenetic landscape. J Biol Chem 293:13795–13804. https://doi.org/10.1074/jbc.R117.001232
37. Ameneiro C, Moreira T, Fuentes-Iglesias A et al (2020) BMAL1 coordinates energy metabolism and differentiation of pluripotent stem cells. Life Sci Alliance 3:e201900534. https://doi.org/10.26508/lsa.201900534
38. Gallardo A, Molina A, Asenjo HG et al (2020) The molecular clock protein Bmal1 regulates cell differentiation in mouse embryonic stem cells. Life Sci Alliance 3:e201900535. https://doi.org/10.26508/lsa.201900535
39. Thakur S, Storewala P, Basak U et al (2020) Clocking the circadian genes in human embryonic stem cells. Stem Cell Investig 7:9. https://doi.org/10.21037/sci-2020-014
40. Koronowski KB, Sassone-Corsi P (2021) Communicating clocks shape circadian homeostasis. Science 371:eabd0951. https://doi.org/10.1126/science.abd0951
41. Balsalobre A, Brown SA, Marcacci L et al (2000) Resetting of circadian time in peripheral tissues by glucocorticoid signaling. Science 289:2344–2347. https://doi.org/10.1126/science.289.5488.2344
42. Yagita K, Okamura H (2000) Forskolin induces circadian gene expression of *rPer1*, *rPer2* and *dbp* in mammalian rat-1 fibroblasts. FEBS Lett 465:79–82. https://doi.org/10.1016/S0014-5793(99)01724-X
43. Verlande A, Masri S (2019) Circadian clocks and cancer: timekeeping governs cellular metabolism. Trends Endocrinol Metab 30:445–458. https://doi.org/10.1016/j.tem.2019.05.001
44. Kiessling S, Beaulieu-Laroche L, Blum ID et al (2017) Enhancing circadian clock function in cancer cells inhibits tumor growth. BMC Biol 15:13. https://doi.org/10.1186/s12915-017-0349-7
45. Ogino T, Matsunaga N, Tanaka T et al (2021) Post-transcriptional repression of circadian component CLOCK regulates cancer-stemness in murine breast cancer cells. Elife 10:e66155. https://doi.org/10.7554/eLife.66155
46. Seron-Ferre M, Valenzuela GJ, Torres-Farfan C (2007) Circadian clocks during embryonic and fetal development. Birth Defect Res C 81:204–214. https://doi.org/10.1002/bdrc.20101
47. Serón-Ferré M, Mendez N, Abarzua-Catalan L et al (2012) Circadian rhythms in the fetus. Mol Cell Endocrinol 349:68–75. https://doi.org/10.1016/j.mce.2011.07.039
48. van der Horst GTJ, Muijtjens M, Kobayashi K et al (1999) Mammalian Cry1 and Cry2 are essential for maintenance of circadian rhythms. Nature 398:627–630. https://doi.org/10.1038/19323
49. Zheng B, Albrecht U, Kaasik K et al (2001) Nonredundant roles of the mPer1 and mPer2 genes in the mammalian circadian clock. Cell 105:683–694. https://doi.org/10.1016/S0092-8674(01)00380-4
50. Kondratov RV, Kondratova AA, Gorbacheva VY et al (2006) Early aging and age-related pathologies in mice deficient in BMAL1, the core component of the circadian clock. Genes Dev 20:1868–1873. https://doi.org/10.1101/gad.1432206
51. DeBruyne JP, Weaver DR, Reppert SM (2007) CLOCK and NPAS2 have overlapping roles in the suprachiasmatic circadian clock. Nat Neurosci 10:543–545. https://doi.org/10.1038/nn1884
52. Hanna J, Cheng AW, Saha K et al (2010) Human embryonic stem cells with biological and epigenetic characteristics similar to those of mouse ESCs. Proc Natl Acad Sci USA 107:9222–9227. https://doi.org/10.1073/pnas.1004584107
53. Ware CB, Nelson AM, Mecham B et al (2014) Derivation of naive human embryonic stem cells. Proc Natl Acad Sci USA 111:4484–4489. https://doi.org/10.1073/pnas.1319738111
54. Okita K, Yamakawa T, Matsumura Y et al (2013) An efficient nonviral method to generate integration-free human-induced pluripotent stem cells from cord blood and peripheral blood cells. Stem Cells 31:458–466. https://doi.org/10.1002/stem.1293